

## Interaction between $\delta$ and $\epsilon$ Subunits of $F_1$ -ATPase from Pig Heart Mitochondria. Circular Dichroism and Intrinsic Fluorescence of Purified and Reconstituted $\delta\epsilon$ Complex<sup>†</sup>

François Penin,\* Gilbert Deléage, Dominique Gagliardi, Bernard Roux, and Danièle C. Gautheron

Laboratoire de Biologie et Technologie des Membranes du CNRS, Université Claude Bernard de Lyon, 43 Bd du 11 Novembre 1918, F-69622 Villeurbanne, France

Received November 30, 1989; Revised Manuscript Received June 26, 1990

**ABSTRACT:** A  $\delta\epsilon$  complex has been purified as a molecular entity from pig heart mitochondrial  $F_1$ -ATPase. This  $\delta\epsilon$  complex has also been reconstituted from purified  $\delta$  and  $\epsilon$  subunits. Both isolated and reconstituted  $\delta\epsilon$  complexes have  $\delta_1\epsilon_1$  stoichiometry and are indistinguishable by their chromatographic behavior, their circular dichroism spectra (CD spectra), and their intrinsic fluorescence features. The content of secondary structures deduced from CD spectra of the  $\delta\epsilon$  complex appears to be the sum of the respective contributions of purified  $\delta$  and  $\epsilon$  subunits. All intrinsic fluorescence studies carried out on isolated  $\epsilon$  subunit and  $\delta\epsilon$  complex show that the single tryptophan residue located on  $\epsilon$  is involved in the interaction between  $\delta$  and  $\epsilon$  subunits. Results obtained with  $F_1$ -ATPase are in favor of the same  $\delta\epsilon$  interaction in the entire enzyme.

In all energy-transducing membranes, ATP is synthesized by the ATPase<sup>1</sup>-ATP synthase complex, a multimeric enzyme consisting of a catalytic part,  $F_1$ , attached to a proton-conducting, transmembranous part,  $F_0$ . One crucial problem for the understanding of the molecular mechanism of ATP synthesis concerns energy transfer between  $F_0$  and  $F_1$ . Hence, knowledge of the structure and the role of the individual subunits that hold  $F_1$  and  $F_0$  complexes together is of great importance.

The mitochondrial  $F_0F_1$ -ATPase (especially the  $F_0$  part) is more complicated than its bacterial and chloroplastic counterparts with respect to polypeptide composition. At least 13 subunits have been identified in mammalian mitochondria [for reviews, see Hatefi (1985), Godinot and Di Pietro (1986), and Walker et al. (1987)], while only eight subunits exist in bacteria [see reviews by Fillingame (1981) and Schneider and Altendorf (1987)]. As does bacterial  $F_1$ , mitochondrial  $F_1$  contains five subunits with  $\alpha_3\beta_3\gamma_1\delta_1\epsilon_1$  stoichiometry [see review by Amzel and Pederson (1983)]. However, only the mitochondrial  $\alpha$ ,  $\beta$ , and  $\gamma$  subunits are the counterparts of the same-named subunits of bacterial  $F_1$ , as shown by primary sequence analysis (Walker et al., 1985). By reconstitution experiments, these three subunits have been shown to be essential in ATP hydrolysis (Yoshida et al., 1977). The  $\beta$  subunit is recognized to play a central role in catalysis and regulation; essential thiols have been localized on  $\alpha$  and  $\gamma$  subunits of the enzyme from *Schizosaccharomyces pombe* (Falson et al., 1986).

The role of mitochondrial  $\delta$  and  $\epsilon$  subunits in the  $F_0F_1$  complex is unknown (Futai et al., 1989). Mitochondrial  $\delta$  subunit exhibits striking sequence homology with bacterial  $\epsilon$  subunit but not with bacterial  $\delta$  subunit. Besides, there seems to be no bacterial or chloroplastic counterpart for mitochondrial  $\epsilon$  subunit (Walker et al., 1982, 1985). Since mitochondrial  $\delta$  subunit is homologous to bacterial  $\epsilon$  subunit, one could suppose a similar function for both proteins. Bacterial  $\epsilon$  subunit has been described to mediate the specific attachment of  $F_1$  to  $F_0$  (Tuttas-Dörschug & Hanstein, 1989) and its

presence is required together with bacterial  $\delta$  subunit for the catalysis of ATP-dependent energy transduction in the reconstituted  $F_0F_1$  complex (Sternweis, 1978).

Although the primary sequences of bovine mitochondrial  $\delta$  subunit (15 065 Da) and  $\epsilon$  subunit (5652 Da) have been determined (Walker et al., 1985), very little information is available about the topology of these subunits in the  $F_0F_1$  complex. Recently, the accessibility of  $\delta$  subunit has been probed in  $F_1$  and in the  $F_0F_1$  complex by using monoclonal antibodies (Lunardi et al., 1989).

In the present study, we show that  $\delta$  and  $\epsilon$  subunits exist as a tight complex that can be purified as a molecular entity from  $F_1$ -ATPase; it exhibits a  $\delta_1\epsilon_1$  stoichiometry. This  $\delta\epsilon$  complex can also be reconstituted from purified  $\delta$  and  $\epsilon$  subunits. It has the same properties as the isolated  $\delta\epsilon$  complex, i.e., the same stoichiometry, identical chromatographic retention times, superimposed circular dichroism spectra, and the same fluorescence properties. A single tryptophan residue is present in pig heart  $F_1$ -ATPase, as in beef heart  $F_1$ -ATPase (Walker et al., 1985). This tryptophan, which is located in the  $\epsilon$  subunit, is of particular interest for the study of  $\delta$ - $\epsilon$  interaction by intrinsic fluorescence methods. We show that this tryptophan, water accessible in isolated  $\epsilon$  subunit, is buried in isolated  $\delta\epsilon$  complex. It is concluded that this tryptophan residue, located within the N-terminal region of  $\epsilon$  subunit, is involved in  $\delta\epsilon$  interaction. Our results indicate that this interaction exists in the whole  $F_1$ -ATPase.

### EXPERIMENTAL PROCEDURES

**Materials.** Gel-filtration HPLC column Protein PAK Glass 200SW and RP-HPLC column Delta PAK C<sub>4</sub>-300 Å were from Waters. Centriprep and Centricon concentrators equipped with YM10 ultrafiltration membranes were from

<sup>1</sup> Abbreviations: ATPase, adenosine-5'-triphosphatase (EC 3.6.1.3);  $F_1$ , solubilized mitochondrial ATPase; SDS, sodium dodecyl sulfate; SDS-PAGE, polyacrylamide gel electrophoresis in the presence of SDS; DTT, dithiothreitol; EDTA, ethylenediaminetetraacetic acid; Tris, 2-amino-2-(hydroxymethyl)propane-1,3-diol; TFA, trifluoroacetic acid; HPLC, high-performance liquid chromatography; CD, circular dichroism.

<sup>†</sup> Financial support by the CNRS, LBTM UM 380024, is acknowledged.

Amicon. Molecular mass marker proteins were from Serva.

**Biological Preparations.** A previously described procedure was used to prepare pig heart mitochondria (Gautheron et al., 1964; Godinot et al., 1969) and purified  $F_1$ -ATPase (nucleotide depleted; Penin et al., 1979). Purified  $\delta$  and  $\epsilon$  subunits from  $F_1$ -ATPase were obtained as described in detail elsewhere (Gagliardi et al., in preparation). In brief,  $F_1$ -ATPase was dissociated into two fractions by cold treatment essentially as described by Williams and Pederson (1986) for the rat liver enzyme. The soluble fraction (containing essentially  $\beta$ ,  $\delta$ , and  $\epsilon$  subunits) was fractionated by anion-exchange chromatography at pH 7.5:  $\delta$  and  $\epsilon$  subunits were not retained on the anion exchanger, while  $\beta$  subunit was retained and further purified. The  $\delta$  and  $\epsilon$  subunits were then separated by reverse-phase HPLC on a Delta PAK  $C_4$  300 Å column by using a linear gradient of acetonitrile in 0.1% trifluoroacetic acid- $H_2O$ . The  $\epsilon$  and  $\delta$  subunits were eluted at 42% and 52% acetonitrile, respectively.

**Analytical Methods.** The protein content was estimated by the method of Lowry et al. (1951). An alternative electrophoretic method was used to estimate the protein contents of  $\delta$  and  $\epsilon$  subunits. This method takes into account the molecular mass of  $F_1$  (371 000 Da) and the  $\alpha_3\beta_3\gamma_1\delta_1\epsilon_1$  stoichiometry of  $F_1$  subunits. SDS-polyacrylamide gel electrophoresis (15% acrylamide) was performed according to Laemmli (1970), as detailed by Penin et al. (1984). The samples of purified  $F_1$ ,  $\delta$  and  $\epsilon$  subunits, and  $\delta\epsilon$  complex were prepared by mixing 50  $\mu$ L of protein solution (containing 15–300  $\mu$ g of protein) with 75  $\mu$ L of 3.5% SDS, 6%  $\beta$ -mercaptoethanol, 35% glycerol, and 100 mM Tris-HCl buffer, pH 6.8. Increasing amounts of dissociated  $F_1$  (10–59  $\mu$ g) were loaded in seven wells of a 15-well gel. The remaining free wells were then loaded with the samples to be analyzed ( $\delta$ ,  $\epsilon$ , or  $\delta\epsilon$  complex). After electrophoresis, the gel was stained with Coomassie blue R250 (Fairbanks et al., 1971) and dried between two cellophane sheets. The spots of  $\delta$  and  $\epsilon$  were then integrated by using a Vernon PHI 6 gel scanner. Standard curves of pmol of  $\delta$  or  $\epsilon$  versus intensity of  $\delta$  or  $\epsilon$  spots were built up from the data of the wells loaded with variable amounts of purified  $F_1$ . The amount of  $\delta$  and/or  $\epsilon$  in samples was then determined by using the respective standard curves for  $\delta$  and  $\epsilon$ . Although this electrophoretic method is time-consuming and standard curves for  $\delta$  and  $\epsilon$  with purified  $F_1$  must be done in each electrophoresis gel, it presents the following definite advantages: (i) amounts of protein as low as 0.5  $\mu$ g for  $\epsilon$  and 1  $\mu$ g for  $\delta$  can be estimated with good accuracy, and (ii) when  $\delta\epsilon$  complex was estimated (see Results), the ratio of spot intensity of the two subunits could be directly compared with that observed in  $F_1$ .

**CD Measurements.** CD spectra were recorded between 195 and 250 nm by using a Jobin-Yvon Mark IV dichrograph, at a constant rate of 1 nm $\cdot$ min $^{-1}$ , and 0.02-cm path length cells. All measurements were made at room temperature. The molar ellipticities were expressed as deg $\cdot$ cm $^2$  $\cdot$ dmol $^{-1}$  on the basis of molecular masses of 15 065 Da for  $\delta$  subunit and 5652 Da for  $\epsilon$  subunit. The mean molecular masses for amino acid residues are 103, 113, and 104 for  $\delta$ ,  $\epsilon$ , and  $\delta\epsilon$  complex, respectively. All these values were deduced from bovine  $F_1$ -ATPase subunit sequences (Walker et al., 1985) since  $\delta$  and  $\epsilon$  subunits from pig heart and beef heart  $F_1$ -ATPase exhibit the same respective apparent molecular masses as determined by SDS-PAGE and similar amino acid analysis (unpublished results). The secondary structure percentages were determined from the measured ellipticities by using a multilinear least-square program based on data proposed by Bolotina et al. (1981a,b)

considering four conformational states ( $\alpha$  helix,  $\beta$  sheet,  $\beta$  turn, and aperiodic conformations). In our program, the sum of the deduced percentages was not constrained to be 100% and each percentage of secondary structure can take any value.

**Fluorescence Measurements.** Fluorescence measurements were carried out at 27 °C in a thermostated quartz cuvette (1  $\times$  1 cm) with a Biologic spectrofluoropolarimeter. Calibrations of excitation and emission wavelengths have been carried out by using *N*-acetyltyrosinamide and *N*-acetyltryptophanamide. A 150-W xenon source was used. Excitation spectra have been corrected for the lamp emission power and the monochromator transmission for each wavelength. For the quenching experiments with acrylamide, 4- $\mu$ L aliquots of an 8 M stock solution were added progressively to 1 mL of protein solution up to a 0.25 M final concentration of acrylamide. A 300-nm excitation wavelength was used to avoid an inner filter effect due to the acrylamide absorbance. Solutions of 0.5–5 M NaI were freshly prepared, containing 10 mM  $Na_2SO_3$  to prevent  $I_3^-$  formation (Lehrer, 1971) and NaCl to bring ionic strength equivalent to 5 M for quenching with iodide. Aliquots of 50  $\mu$ L of these solutions were added to 1.1-mL protein samples.

Stern-Volmer plots were drawn by using the classical equation:

$$F_0/F = 1 + K_{SV}Q$$

where  $F_0$  and  $F$  are the fluorescence intensities in the absence and presence of the quencher, respectively, and  $Q$  is the molar concentration of the quenching agent.  $K_{SV}$  is the Stern-Volmer quenching constant of the accessible fluorophore.  $K_{SV}$  is the product of the fluorescence lifetime ( $\tau$ ) and the rate constant for quenching ( $k_Q$ ). To estimate the accessible fluorophore fraction  $f_a$  in  $F_1$ -ATPase, modified Stern-Volmer plots were used, according to the relation (Lehrer, 1971)

$$F_0/(F_0 - F) = 1/f_a + 1/(f_a K_Q Q)$$

where  $K_Q$  is the quenching constant. All the fluorescence values have been corrected for background and dilution. The assay solution's absorbance was always chosen lower than 0.05 cm $^{-1}$  at the excitation wavelengths used to avoid inner filter effects.

## RESULTS

Figure 1 represents the purification by gel filtration of  $\delta\epsilon$  complex (Figure 1A) and of reconstituted  $\delta\epsilon$  complex (Figure 1B). Electrophoretic analysis of these complexes by SDS-PAGE is given in Figure 1C (lanes 5 and 6) and compared with purified  $F_1$ -ATPase,  $\delta$  subunit, and  $\epsilon$  subunit (lanes 1, 2, and 3, respectively).

**Purification of  $\delta\epsilon$  Complex.** In the course of purification of  $\delta$  and  $\epsilon$  subunits from  $F_1$ -ATPase (see Experimental Procedures), the fraction that is not retained on the anion exchanger, which contained  $\delta$  and  $\epsilon$  subunits, was concentrated by ultrafiltration with a Centriprep equipped with a YM10 membrane. An electrophoretic profile of the concentrate is shown in Figure 1C (lane 4). This concentrate was then submitted to gel filtration on a 200SW column equilibrated with 100 mM sodium phosphate and 2 mM DTT buffer, pH 7.0. Figure 1A shows a typical elution profile. The major peak (peak a3) is exclusively composed of purified  $\delta\epsilon$  complex, as shown in Figure 1C, lane 5. When necessary, fraction a3 was concentrated by ultrafiltration with a Centricon equipped with a YM10 membrane. Electrophoretic analyses, not reported here, have shown that peak a1 (exclusion volume) contains aggregated  $\alpha$  and  $\gamma$  subunits of  $F_1$  while peak a2 contains some  $\beta$  subunit. No protein was detected in peaks a4 and a5.

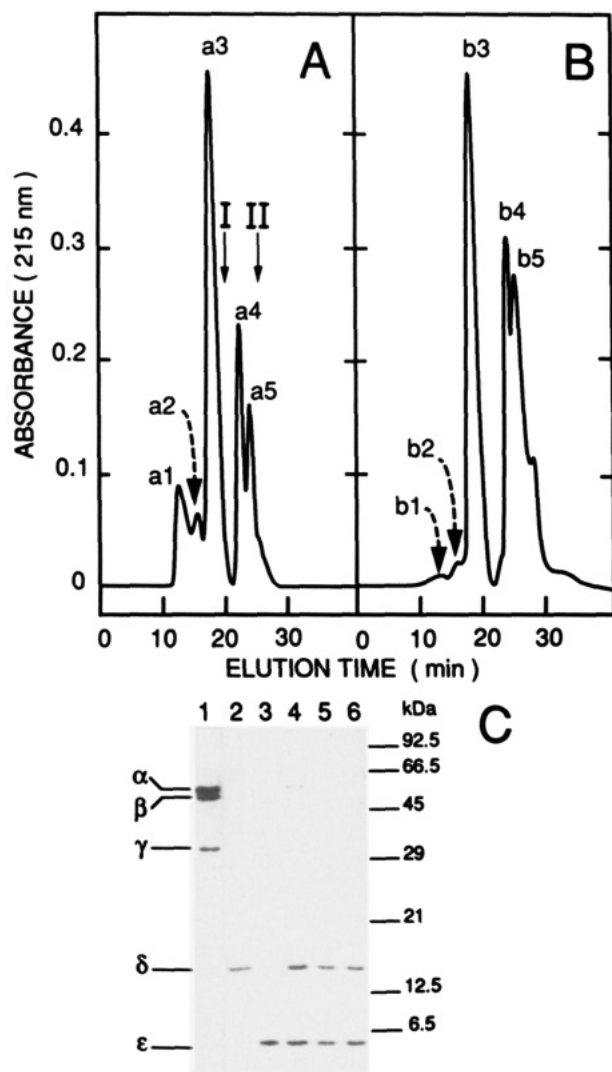


**FIGURE 1:** Purification of  $\delta\epsilon$  complex by filtration on a 200SW column and electrophoretic analysis. (A) A concentrated fraction containing  $\delta$  and  $\epsilon$  subunits (see the text) was filtered by HPLC on a Protein PAK Glass 200SW column ( $0.8 \times 30$  cm) in 100 mM sodium phosphate and 2 mM DTT buffer, pH 7.0; sample volume 300  $\mu$ L, containing 1 mg of protein; flow rate 0.5 mL/min. Main peaks are numbered from a1 to a5. Arrows numbered I and II indicate the retention times of purified  $\delta$  and  $\epsilon$  subunits, respectively, under the same chromatographic conditions. (B) Purified  $\delta$  subunit (500  $\mu$ g) and  $\epsilon$  subunit (300  $\mu$ g) were mixed in 100 mM sodium phosphate and 2 mM DTT buffer, pH 7.0, for 10 min and filtered on the 200SW column as in (A). Main peaks are numbered from b1 to b5. (C) SDS-polyacrylamide gel electrophoresis. Lane 1: purified  $F_1F_0$ -ATPase (14  $\mu$ g); from top to bottom, subunits  $\alpha$ ,  $\beta$ ,  $\gamma$ ,  $\delta$ , and  $\epsilon$ . Lane 2: purified  $\delta$  subunit (1.5  $\mu$ g). Lane 3: purified  $\epsilon$  subunit (1.5  $\mu$ g). Lane 4: concentrated fraction loaded on 200SW column in chromatography A (7  $\mu$ g). Lane 5: peak a3 of chromatography A (4  $\mu$ g). Lane 6: peak b3 of chromatography B (4  $\mu$ g). Migrations of known molecular mass proteins are indicated on the right of the figure. Conditions of electrophoresis are described under Experimental Procedures.

Arrows I and II in Figure 1A indicate the retention times for purified  $\delta$  and  $\epsilon$  subunits, respectively, under the same chromatographic conditions. Electrophoretic profiles of purified  $\delta$  and  $\epsilon$  subunits are presented in Figure 1C (lanes 2 and 3).

**Stoichiometry and Stability of  $\delta\epsilon$  Complex.** After calibration of the 200SW column under the above conditions with standard proteins, the apparent molecular masses of  $\delta\epsilon$  complex and purified  $\delta$  subunit were, respectively, 31 000 and 23 000 Da; the retention time for  $\epsilon$  was out of range of the calibration curve.

To determine the stoichiometry of  $\delta$  and  $\epsilon$  in the  $\delta\epsilon$  complex, the electrophoretic method of protein assay detailed under

Experimental Procedures was used: a molecular ratio  $\delta/\epsilon$  of  $1.06 \pm 0.05$  has been measured for purified  $\delta\epsilon$  complex, as compared to the stoichiometry  $\delta_1\epsilon_1$  in  $F_1$ -ATPase. It should be mentioned that before filtration of the above concentrate on the 200SW column (Figure 1C, lane 4) the molecular ratio  $\delta/\epsilon$  was  $1.02 \pm 0.05$ . This indicates that no significant dissociation of the  $\delta\epsilon$  complex occurred during purification. Taking into account the molecular mass of  $\delta\epsilon$  complex (20 700 Da) and the minimal concentration of protein assayed (0.05 mg/mL; 200  $\mu$ L injected on 200SW column), it can be deduced that the dissociation constant of  $\delta$ - $\epsilon$  interaction is lower than  $5 \times 10^{-6}$  M under the conditions used at pH 7.0.

It should be mentioned that when purification of  $\delta\epsilon$  complex was performed at a pH below 5.0, the  $\delta/\epsilon$  molecular ratio was less than unity and some free  $\epsilon$  was detected. Conversely, when the pH was above 7.0, the  $\delta/\epsilon$  molecular ratio was higher than unity and no free  $\epsilon$  was detected. These results are explained by nonspecific interactions of  $\delta$  and  $\epsilon$  subunits with the column phase as a function of pH. Indeed, when purified  $\delta$  subunit was filtered on the 200SW column at a pH below 5.0, its recovery decreased; for purified  $\epsilon$ , a decrease of its recovery was observed when filtration was performed at a pH above 7.0. Thus, purification of  $\delta\epsilon$  complex by filtration on the 200SW column at pH 7.0 as described above appears to be a good condition to avoid artifactual dissociation of  $\delta\epsilon$  complex. For clarity, the purified  $\delta\epsilon$  complex will be named "isolated  $\delta\epsilon$  complex" in the following.

It should be added that  $\delta\epsilon$  complex was not significantly dissociated when analyzed either by isoelectric focusing (pI of  $\delta\epsilon$  complex: 5.9) or by electrophoresis on a polyacrylamide gel without SDS (data not shown).

**Reconstitution of  $\delta\epsilon$  Complex.** Purified  $\delta$  subunit was mixed for 5 min with an excess of purified  $\epsilon$  subunit in 0.1 M sodium phosphate and 1 mM DTT buffer, pH 7.0, and the solution was submitted to gel filtration on the 200 SW column (Figure 1B) to eliminate free  $\epsilon$  subunit (purified  $\epsilon$  subunit was added in excess in order to avoid the presence of free  $\delta$  subunit, which is not well separated from  $\delta\epsilon$  complex by gel filtration). This is shown by their respective retention times in Figure 1A. The major peak b3 contained reconstituted  $\delta\epsilon$  complex as shown by electrophoresis (Figure 1C, lane 6). Electrophoretic analyses not reported here have shown that peak b1 contained aggregated  $\delta$  subunits and peak b2 contained  $\delta$  and  $\epsilon$  subunits (possibly oligomers of the  $\delta\epsilon$  complex); free  $\epsilon$  subunit was eluted in peak b5. A molar ratio  $\delta/\epsilon$  of  $1.01 \pm 0.05$  has been determined for reconstituted  $\delta\epsilon$  complex, by using the electrophoretic method of protein assay described under Experimental Procedures. Hence, reconstituted  $\delta\epsilon$  complex exhibits the same chromatographic behavior and the same stoichiometry as isolated  $\delta\epsilon$  complex.

**Circular Dichroism Spectra of Purified  $\delta$  and  $\epsilon$  Subunits and of  $\delta\epsilon$  Complex.** The CD spectra shown in Figure 2 have been obtained with purified  $\delta$  (Figure 2A) and  $\epsilon$  subunits (Figure 2B). The contributions of the different secondary structures determined by using the model of Bolotina et al. (1981a) are give in Table I. Figure 2, panels C and D show the spectra recorded for isolated and reconstituted  $\delta\epsilon$  complexes, respectively. They are very similar, as confirmed by the analysis of the contributions of the secondary structures (Table I). Although the program was not constrained (see Experimental Procedures), the sum of these contributions is close to 100%, except for the  $\epsilon$  subunit, where it is 121%. However, all the percentages are between 0 and 100%, indicating no need to constrain the program. Moreover, the fit between experimental data and calculated ellipticities from

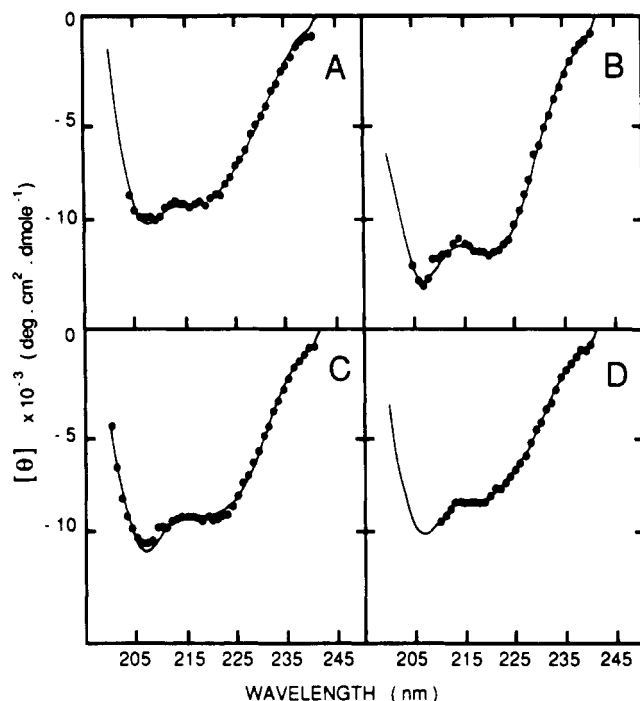


FIGURE 2: Circular dichroism spectra of purified  $\delta$  subunit,  $\epsilon$  subunit, and isolated or reconstituted  $\delta\epsilon$  complex. Spectra were recorded as described under Experimental Procedures. Closed circles are experimental data; solid lines are spectra computed by using calculated percentages of secondary structures given in Table I. (A)  $\delta$  subunit, 0.8 mg/mL; (B)  $\epsilon$  subunit, 1 mg/mL; (C) isolated  $\delta\epsilon$  complex, 0.7 mg/mL; (D) reconstituted  $\delta\epsilon$  complex, 0.3 mg/mL. All samples are in 0.1 M sodium phosphate and 2 mM DTT buffer, pH 7.0, except for  $\epsilon$  subunit, for which the buffer pH was 6.0.

Table I: Calculated Percentages of Secondary Structure for  $\delta$  and  $\epsilon$  Subunits and for  $\delta\epsilon$  Complex<sup>a</sup>

	% of secondary structure				
	$\alpha$ helix	$\beta$ sheet	$\beta$ turn	aperiodic	sum
$\delta$ subunit	26 (0.5)	14 (0.6)	15 (0.6)	43 (2)	98
$\epsilon$ subunit	29 (0.7)	13 (0.8)	14 (1)	65 (3)	121
isolated $\delta\epsilon$ complex	25 (0.4)	10 (0.7)	14 (0.6)	53 (1)	102
reconstituted $\delta\epsilon$ complex	23 (0.3)	13 (0.3)	15 (0.5)	49 (3)	100

<sup>a</sup>The indicated percentages were obtained from the unconstrained program without further adjustment (see Experimental Procedures). Calculations were made according to Bolotina et al. (1981a,b) from the circular dichroism spectra in Figure 2. The conditions are the same as in Figure 2. Standard deviations from the theoretical model are given in parentheses.

the percentages given in Table I are very good in all cases. All these features indicate the validity of the procedure; this was already pointed out by Brahm and Brahm (1980). Therefore, the secondary structure of the reconstituted  $\delta\epsilon$  complex looks like that of isolated  $\delta\epsilon$  complex.

**Intrinsic Fluorescence of Purified  $\delta$  and  $\epsilon$  Subunits.** The fluorescence spectra are given in Figure 3 for the  $\delta$  and  $\epsilon$  subunits. The excitation spectrum of the  $\delta$  subunit exhibits a maximum near 280 nm (Figure 3A, solid line), whereas in the case of  $\epsilon$  subunit, the maximum is centered around 288 nm with a shoulder at 280 nm (Figure 3A, dashed line). The emission spectrum presents a maximum at 310 nm for  $\delta$  subunit (Figure 3B, solid line), which is close to that observed with *N*-acetyltyrosinamide (not shown). Hence, the fluorescence of the  $\delta$  subunit is due to its single tyrosine residue. In the case of  $\epsilon$  subunit, the maximum of emission is at 350 nm (Figure 3B, dashed line), which is close to that observed with *N*-acetyltryptophanamide (not shown). This typical

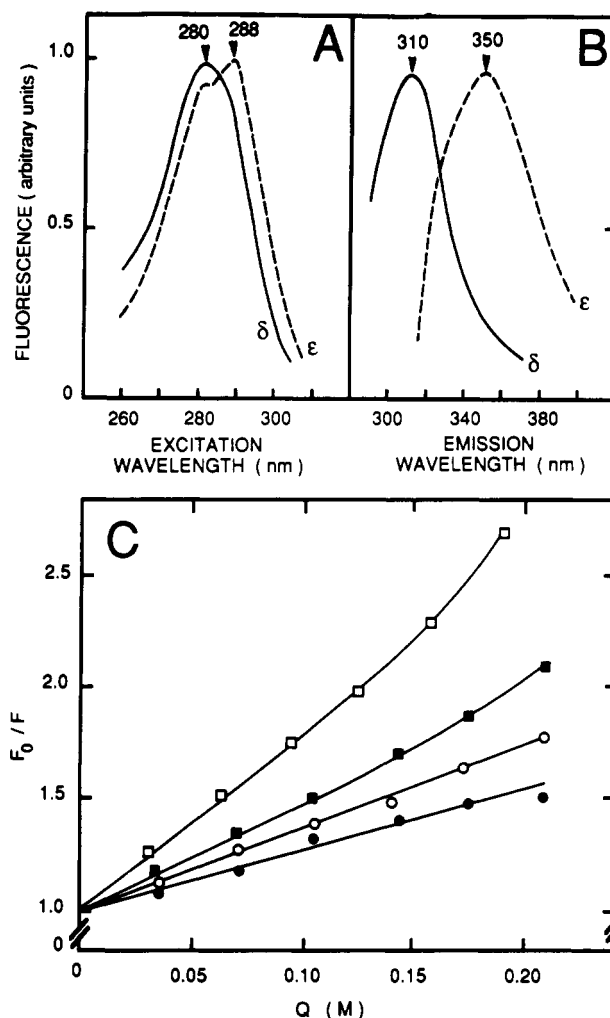


FIGURE 3: Intrinsic fluorescence of purified  $\delta$  and  $\epsilon$  subunits. The  $\delta$  subunit (0.8 mg/mL) and  $\epsilon$  subunit (1 mg/mL) were in 0.1 M sodium phosphate and 2 mM DTT buffer at pH 7.0 and pH 6.0, respectively. (A) Fluorescence excitation spectra of  $\delta$  subunit (solid line) or  $\epsilon$  subunit (dashed line). The emission wavelength was set up at 330 and 344 nm for  $\delta$  and  $\epsilon$  subunits, respectively. (B) Fluorescence emission spectra of  $\delta$  subunit (solid line) and  $\epsilon$  subunit (dashed line). The excitation wavelength was set up at 276 and 294 nm for  $\delta$  and  $\epsilon$  subunits, respectively. The positions of the maxima in excitation (A) and emission (B) are indicated by arrows. (C) Stern-Volmer plots of  $\epsilon$  subunit with iodide ( $\bullet$ ) and acrylamide ( $\blacksquare$ ) as quenching agents. The open symbols are for denatured  $\epsilon$  subunit with iodide ( $\circ$ ) and acrylamide ( $\square$ ) as quenching agents. Denaturation of the  $\epsilon$  subunit was obtained with 6 M guanidine hydrochloride in the above medium. Fluorescence measurements were carried out as described under Experimental Procedures.

fluorescence is due to the single tryptophan present in  $\epsilon$  subunit. The emission spectrum of  $\epsilon$  subunit is not modified upon addition of guanidine hydrochloride (not shown), indicating that the tryptophan is accessible to the solvent rather than buried within the protein. To estimate the degree of accessibility of this tryptophan residue, fluorescence quenching experiments were carried out with acrylamide and iodide as quenching agents. Iodide is a large, polar anion and is considered to have access only to surface tryptophan residues. Polar, nonionic acrylamide has good access to all tryptophan residues but those buried into the hydrophobic core of the protein (Lehrer, 1971; Eftink & Ghiron, 1976; Lehrer & Leavis, 1978). Stern-Volmer plots for the  $\epsilon$  subunit are shown in Figure 3C. As expected, the efficiency of quenching is greater for acrylamide than for iodide. Although a higher accessibility of tryptophan is observed for the denatured state than for the native form, the low difference between the  $K_{SV}$  values (Table II) confirms

Table II: Stern-Volmer Quenching Constants of Tryptophan in  $\epsilon$  Subunit and  $\delta\epsilon$  Complex<sup>a</sup>

	$K_{SV}$ (iodide) ( $M^{-1}$ )	$K_{SV}$ (acrylamide) ( $M^{-1}$ )
native $\epsilon$ subunit	2.9	5
denatured $\epsilon$ subunit	3.8	7.8
native $\delta\epsilon$ complex <sup>b</sup>	1.7	2.6
denatured $\delta\epsilon$ complex	3.6	7.9

<sup>a</sup>The quenching constants were deduced from the initial slopes of the Stern-Volmer plots presented in Figures 3 and 4. <sup>b</sup>Isolated or reconstituted.

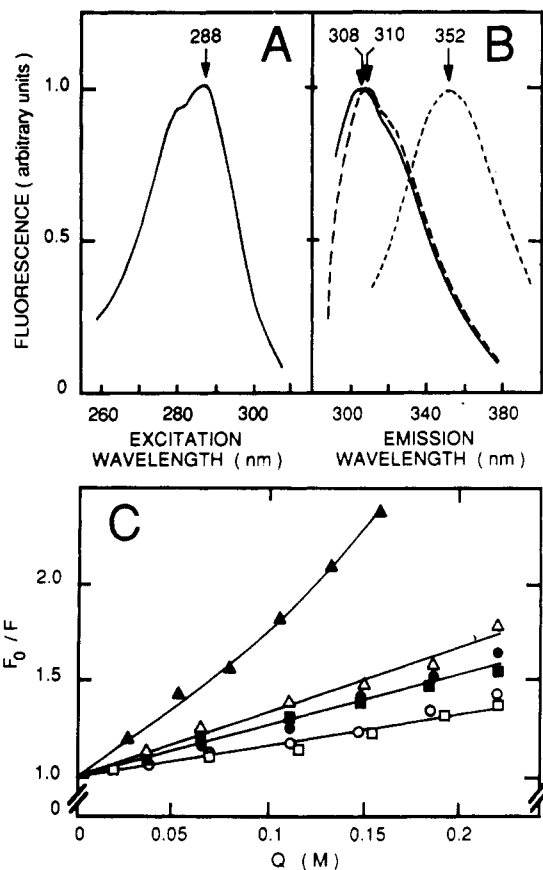


FIGURE 4: Intrinsic fluorescence of isolated and reconstituted  $\delta\epsilon$  complex. The isolated or reconstituted  $\delta\epsilon$  complexes (0.3 mg/mL) were in 0.1 M sodium phosphate and 2 mM DTT buffer, pH 7.0. (A) Fluorescence excitation spectra of isolated or reconstituted  $\delta\epsilon$  complexes. The emission wavelength was set up at 344 nm. (B) Fluorescence emission spectra of native  $\delta\epsilon$  complex, isolated (solid line) or reconstituted (dashed line). The excitation wavelengths were set up at 294 nm. The spectrum shown by the dotted line has been obtained after addition of solid guanidine hydrochloride up to 6 M in the above medium with either isolated or reconstituted  $\delta\epsilon$  complexes. Under these denaturing conditions, the excitation wavelength was also 294 nm. The positions of the maxima in excitation (A) or emission (B) are indicated by arrows. (C) Stern-Volmer plots of either native  $\delta\epsilon$  complexes ( $\square$  and  $\blacksquare$ , isolated;  $\circ$  and  $\bullet$ , reconstituted) or denatured  $\delta\epsilon$  complex ( $\triangle$ ,  $\blacktriangle$ ) with iodide (open symbols:  $\square$ ,  $\circ$ , and  $\triangle$ ) or acrylamide (closed symbols:  $\blacksquare$ ,  $\bullet$ , and  $\blacktriangle$ ) as quenching agents.

the exposed position of the tryptophan in the purified  $\epsilon$  subunit.

**Intrinsic Fluorescence of Isolated or Reconstituted  $\delta\epsilon$  Complex.** Figure 4A shows that the fluorescence spectra of isolated and reconstituted  $\delta\epsilon$  complex are the same. The excitation maximum is observed at about 288 nm with a shoulder at 280 nm, as for  $\epsilon$  subunit. Figure 4B shows that the emission spectra of isolated  $\delta\epsilon$  complex (solid line) and reconstituted  $\delta\epsilon$  complex (dashed line) are very similar, exhibiting a maximum fluorescence at 308–310 nm and a small shoulder at about 320 nm. After denaturation of  $\delta\epsilon$  complex with guanidine hydrochloride, the maximum of emission fluorescence

Table III: Comparison between Tryptophan Fluorescence Yield in Isolated  $\epsilon$  Subunit and  $\delta\epsilon$  Complex<sup>a</sup>

	area of emission spectra (arbitrary units)	fluorescence yield (%)
native $\delta$ subunit <sup>b</sup>	<sup>c</sup>	
native $\epsilon$ subunit <sup>d</sup>	620	100
$\delta + \epsilon$ subunits <sup>e</sup> (numeric sum)	620	100
native $\delta\epsilon$ complex <sup>f</sup>	215	35
denatured $\delta\epsilon$ complex <sup>g</sup>	595	96

<sup>a</sup>Tryptophan fluorescence was estimated from the area of emission spectra between 305 and 450 nm. Excitation wavelength was set up at 294 nm in all cases. In order to allow a quantitative comparison, integration values of fluorescence spectra were corrected for the same protein concentration (10  $\mu$ M) for isolated  $\delta$  and  $\epsilon$  subunits (15 065 and 5652 Da, respectively) and for  $\delta\epsilon$  complex (20 717 Da). <sup>b</sup>When excited at 294 nm, emission spectrum of  $\delta$  subunit was close to fluorescence background. <sup>c</sup>Negligible. <sup>d</sup>The fluorescence spectrum of  $\epsilon$  subunit was taken as 100% tryptophan fluorescence yield. <sup>e</sup> $\delta + \epsilon$  represents the sum of the spectra areas for  $\delta$  and  $\epsilon$  subunits. <sup>f</sup>Since the areas measured for isolated and reconstituted  $\delta\epsilon$  complexes were quite similar, their average value is given here. <sup>g</sup>Denaturation of the  $\delta\epsilon$  complex was obtained with 6 M guanidine hydrochloride as described in the legend to Figure 4.

is centered at 352 nm, as expected for a tryptophan (Figure 4B, dotted line). Therefore, since tryptophan is the only residue with a significant extinction at 294 nm, the tryptophan signal appears to be strongly blue-shifted in the  $\delta\epsilon$  complex. The interaction of  $\epsilon$  and  $\delta$  subunits greatly affects the fluorescence properties of the tryptophan residue present in  $\epsilon$  subunit. Thus, the wavelength of the maximum of the fluorescence emission can be used to monitor the specific interaction between the two subunits.

In order to see whether the tryptophan fluorescence yield of  $\epsilon$  subunit is modified in  $\delta\epsilon$  complex, the actual area of emission spectra (recorded between 305 and 450 nm) of  $\delta$  subunit,  $\epsilon$  subunit, and native or denatured  $\delta\epsilon$  complex have been compared in a quantitative manner. The results given in Table III show that the tryptophan fluorescence yield, taken as 100% for  $\epsilon$  subunit, strongly decreases to 35% for both isolated and reconstituted  $\delta\epsilon$  complexes. As expected, denatured  $\delta\epsilon$  complex exhibits a fluorescence yield (96%) very similar to that of  $\epsilon$  subunit alone.

Figure 4 also shows the Stern-Volmer plots obtained for acrylamide and iodide quenchers in the case of native  $\delta\epsilon$  complexes (isolated or reconstituted) and the denatured complex (Figure 4C). No significant difference is observed between isolated and reconstituted  $\delta\epsilon$  complexes. For a given quencher, the Stern-Volmer quenching constants  $K_{SV}$  (Table II) are lower for the native  $\delta\epsilon$  complex than for the native  $\epsilon$  subunit. Therefore, the tryptophan residue is less accessible in the  $\delta\epsilon$  complex than in the  $\epsilon$  subunit alone. On the contrary, when  $\delta\epsilon$  complexes are denatured, these  $K_{SV}$  values are very close. From modified Stern-Volmer plots (Lehrer, 1971), one can extrapolate the accessible fraction of fluorophore to quencher (data not shown). In all cases,  $f_a$  is equal to 1; i.e., only one class of tryptophan is observed, indicating the presence of only one molecular species of  $\delta\epsilon$  complex.

**Intrinsic Fluorescence of  $F_1$ -ATPase.** The native  $F_1$ -ATPase excitation spectrum shows a maximum around 276 nm (Figure 5A), and its emission spectrum shows a peak centered at 308 nm (Figure 5B, solid line). No typical emission peak due to tryptophan could be detected, even when the excitation wavelength was set up in the range 294–304 nm (data not shown). In contrast, the emission spectra of denatured  $F_1$ -ATPase reported in Figure 5B (dotted and dashed lines) show that, for an excitation wavelength of 294 nm, a shoulder ap-

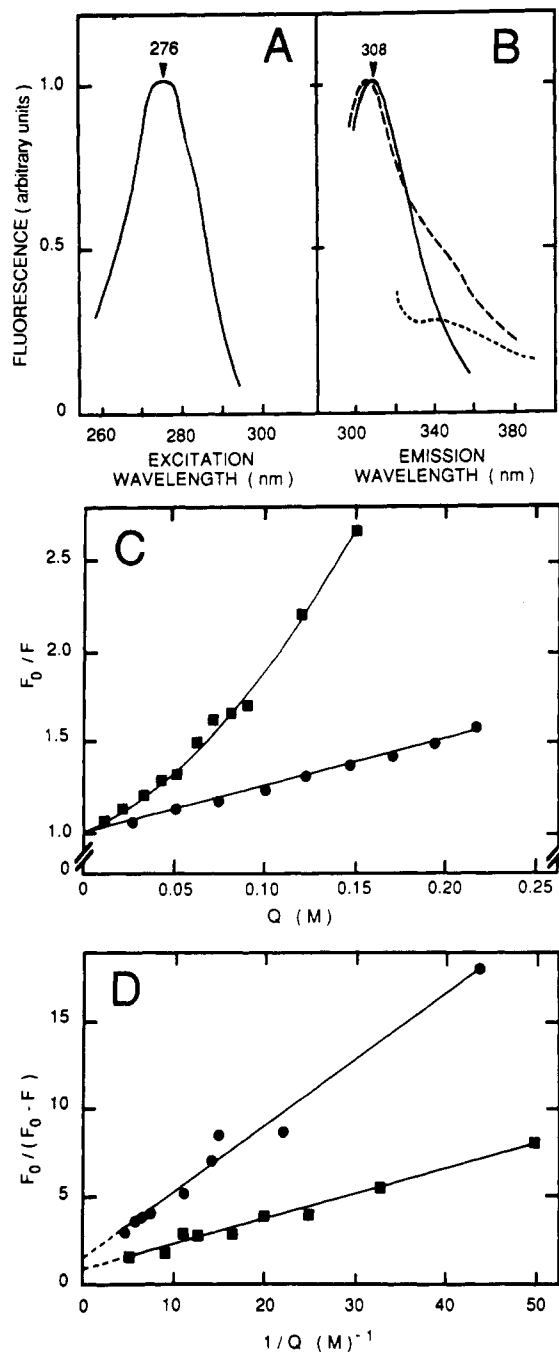


FIGURE 5: Intrinsic fluorescence of  $F_1$ -ATPase.  $F_1$ -ATPase (stock solution) was diluted to 0.7 mg/mL in 5% glycerol, 0.5 mM EDTA, and 5 mM Tris- $H_2SO_4$  buffer, pH 8.0. Denaturation of  $F_1$ -ATPase was achieved after 24 h incubation in the above medium containing 6 M guanidine hydrochloride and 50 mM DTT. (A) Excitation spectrum with emission fluorescence collected at 340 nm. (B) Emission spectra of native  $F_1$ -ATPase (solid line) and denatured  $F_1$ -ATPase (dashed and dotted lines). The excitation wavelengths were 284 nm (solid line), 294 nm (dashed line), and 304 nm (dotted line). (C) Stern-Volmer plot and (D) modified Stern-Volmer plot of native (●) or denatured (■)  $F_1$ -ATPase with acrylamide as quenching agent.

peaks around 340 nm; for an excitation wavelength of 304 nm, a small peak around 345 nm is visible. This peak can be assigned to the fluorescence of the single tryptophan of the  $\epsilon$  subunit, since we have verified that there is no tryptophan present in any other  $F_1$ -ATPase subunits. This was checked by fluorescence under denaturing conditions (data not shown). Quenching experiments performed on native and denatured  $F_1$ -ATPase with acrylamide are reported in Figure 5, panels C and D. It was deduced from Stern-Volmer plots (Figure 5C) that the estimated  $K_{SV}$  values were 2.8 and 7  $M^{-1}$  for

native and denatured  $F_1$ -ATPase, respectively. Besides, it was deduced from modified Stern-Volmer plots (Figure 5D) that 70% of the fluorophores were accessible to acrylamide in  $F_1$ -ATPase ( $1/f_a = 1.4$ ) while all the fluorophores were accessible in the denatured enzyme ( $1/f_a = 1$ ). It should be added that acrylamide has little effect on  $F_1$ -ATPase activity. Indeed, inhibition was only 20% at 0.2 M acrylamide (data not shown). Quenching experiments with iodide have not been possible because  $F_1$ -ATPase precipitates at the NaI concentrations used.

## DISCUSSION

As far as we know, this study is the first demonstration that mitochondrial  $\delta$  and  $\epsilon$  subunits form a tight complex that can be purified from  $F_1$ -ATPase as a molecular entity. Our results indicate that such a  $\delta\epsilon$  complex exists in  $F_1$ -ATPase. It is worth mentioning that Baird and Hammes (1977) had shown the proximity of  $\delta$  and  $\epsilon$  subunits in whole  $F_1$  by cross-linking experiments.

The interaction between  $\delta$  and  $\epsilon$  is strong at neutral pH ( $K_d < 5 \times 10^{-6}$  M). Under acidic conditions (i.e., 0.1% TFA), the interaction is broken, which further allows isolation and purification of each subunit. The  $\delta\epsilon$  complex has a molar ratio  $\delta/\epsilon$  of 1, as determined by comparative electrophoresis with purified  $F_1$  as a reference of  $\alpha_3\beta_3\gamma_1\epsilon_1$  stoichiometry. Although the molecular mass of  $\delta$  subunit is about 15 000 Da, its apparent molecular mass measured by gel-filtration HPLC is 23 000 Da. Besides, the apparent molecular mass of  $\delta\epsilon$  complex is 31 000 Da. The difference between these two apparent masses accounts for the presence of only one  $\epsilon$  subunit (molecular mass about 5 600 Da). Since the molecular ratio  $\delta/\epsilon$  is 1, these results are best explained by a  $\delta_1\epsilon_1$  stoichiometry in the case of the  $\delta\epsilon$  complex.

A  $\delta\epsilon$  complex can also be obtained spontaneously after incubation of purified  $\delta$  and  $\epsilon$  subunits. This reconstituted  $\delta\epsilon$  complex has the same chromatographic behavior as the purified one (Figure 1) and also has a  $\delta_1\epsilon_1$  stoichiometry. Moreover, isolated and reconstituted  $\delta\epsilon$  complexes present very similar structural features, as demonstrated by circular dichroism spectra (Figure 2) and intrinsic fluorescence properties (Figure 4). This shows that  $\delta$  and  $\epsilon$  subunits purified by reverse-phase HPLC have kept their potentiality of reassociation. Besides, they present circular dichroism spectra typical of folded proteins, with helicities in the same range (25–30%) as the  $\delta\epsilon$  complex. Thus, the interaction between the two subunits does not lead to great changes at the level of secondary structures.

In the purified  $\epsilon$  subunit, the tryptophan appears to be quite accessible to the solvent, as shown by comparison of fluorescence data obtained for native and denatured states (Figure 3): identical positions of maxima in fluorescence emission spectra (350 nm) and low differences between quenching constants. On the contrary, this tryptophan is buried in the native  $\delta\epsilon$  complex, since the position of the maximum of emission spectra is blue-shifted up to 30–40 nm as compared to that of  $\epsilon$  subunit alone (Figure 3B) or denatured  $\delta\epsilon$  complex (Figure 4B). Moreover the quenching constant  $K_{SV}$  is lower for native  $\delta\epsilon$  complex than for native  $\epsilon$  subunit (Table II). Although it cannot be decided whether the fluorescence lifetime ( $\tau$ ) or the rate constant ( $k_Q$ ) or both are modified in  $K_{SV}$ , the fact that the fluorescence yield of the tryptophan in the  $\epsilon$  subunit is diminished by 65% in the  $\delta\epsilon$  complex (Table III) suggests the main contribution of a fluorescence lifetime change. All these results indicate that a change in tryptophan environment from a polar region in isolated  $\epsilon$  subunit to a nonpolar region occurs upon formation of the  $\delta\epsilon$  complex.



This study shows the involvement of a tryptophan residue in the strong interaction between  $\delta$  and  $\epsilon$  subunits. Moreover, a partial amino acid sequence of the N-terminal side of the  $\epsilon$  subunit (unpublished results) has revealed that this tryptophan occupies the fourth position, as in beef heart mitochondrial  $\epsilon$  subunit (Walker et al., 1985). Therefore, this N-terminal region of the  $\epsilon$  subunit is likely to be involved in  $\delta\epsilon$  association.

As previously reported for beef heart (Tiedge et al., 1982; Baracca et al., 1986), the native pig heart  $F_1$ -ATPase has a fluorescence emission spectrum typical of tyrosine residues (Keira et al., 1978; this study, Figure 5). We show here that the tryptophan in the  $\epsilon$  subunit can be detected only upon denaturation of  $F_1$ -ATPase. Although the fluorescence of this single tryptophan may be masked by that of the hundreds of tyrosines present in the enzyme, it is more attractive to think that it is blue-shifted and quenched in a manner similar to that in  $\delta\epsilon$  complex. Therefore, the involvement of the tryptophan in the interaction between  $\delta$  and  $\epsilon$  could be the same in the  $\delta\epsilon$  complex either isolated or integrated in  $F_1$ -ATPase.

From a structural point of view, the present study shows that the  $\delta\epsilon$  complex should be treated as a molecular entity of all the  $F_0F_1$  complex. One can wonder what is the functional meaning of such a tight  $\delta\epsilon$  complex: does it have a role similar to OSCP (oligomycin-sensitivity conferring protein; Mac Lennan & Tzagoloff, 1968), which is known to adjust the fitting of  $F_1$  to  $F_0$  for a correct channeling of protons for efficient ATP synthesis (Penin et al., 1986)? Is this  $\delta\epsilon$  complex more directly involved than OSCP in proton transfer between  $F_0$  and  $F_1$ ? Does it give special structural features in the functional asymmetry of  $F_1$ -ATPase (Gautheron et al., 1984)? Work is in progress to obtain functional and structural information in order to elucidate the involvement of these small subunits in  $F_0F_1$  complex activities.

#### ACKNOWLEDGMENTS

Thanks are due to Professor C. Helene and Dr. T. Montenay-Garestier for their helpful criticisms for fluorescence experiments and for final discussion. Thanks are also due to A. Di Pietro for useful suggestions, to C. Van Herwege for the artwork, to C. Brison for typing the manuscript, and to I. Royaud for correcting the spelling mistakes.

**Registry No.** ATPase, 9000-83-3; tryptophan, 73-22-3.

#### REFERENCES

- Amzel, L. M., & Pederson, P. L. (1983) *Annu. Rev. Biochem.* **52**, 801–824.
- Baird, B. A., & Hammes, G. G. (1977) *J. Biol. Chem.* **252**, 4743–4748.
- Baracca, A., Curatola, G., Parenti Castelli, G., & Solaini, S. (1986) *Biochem. Biophys. Res. Commun.* **136**, 891–898.
- Bolotina, I. A., Chekov, V. O., Lugauska, V. Yu, Finkelstein, A. V., & Ptitsyn, O. B. (1981a) *Mol. Biol. (Engl. Transl.)* **14**, 701–708.
- Bolotina, I. A., Chekov, V. O., Lugauska, V. Yu, Finkelstein, A. V., & Ptitsyn, O. B. (1981b) *Mol. Biol. (Engl. Transl.)* **14**, 709–714.
- Brahms, S., & Brahms, J. (1980) *J. Mol. Biol.* **138**, 149–178.
- Eftink, M. R., & Ghiron, C. A. (1976) *Biochemistry* **15**, 672–680.
- Fairbanks, G., Steck, T. L., & Wallach, D. F. H. (1971) *Biochemistry* **10**, 2606–2617.
- Falson, P., Di Pietro, A., & Gautheron, D. C. (1986) *J. Biol. Chem.* **261**, 7151–7159.
- Fillingame, R. H. (1981) *Curr. Top. Bioenerg.* **11**, 35–106.
- Futai, M., Noumi, T., & Maeda, M. (1989) *Annu. Rev. Biochem.* **58**, 111–136.
- Gautheron, D. C., Durand, R., Pialoux, N., & Gaudemer, Y. (1964) *Bull. Soc. Chim. Biol.* **46**, 645–660.
- Gautheron, D. C., Di Pietro, A., Penin, F., Moradi-Améli, M., Fellous, G., & Godinot, C. (1984) in *H<sup>+</sup>-ATPase (ATP synthase): Structure, Function, Regulation* (Papa, S., Altendorf, K., Ernster, L., & Packer, L., Eds.) pp 219–228, Adriatica Editrice, Bari, Italy.
- Godinot, C., & Di Pietro, A. (1986) *Biochimie* **68**, 367–374.
- Godinot, C., Vial, C., Font, B., & Gautheron, D. C. (1969) *Eur. J. Biochem.* **8**, 385–394.
- Hatefi, Y. (1985) *Annu. Rev. Biochem.* **54**, 1015–1069.
- Keira, T., Godinot, C., & Gautheron, D. C. (1978) *Experientia* **34**, 1548–1549.
- Laemmli, U. K. (1970) *Nature* **227**, 680–685.
- Lehrer, S. S. (1971) *Biochemistry* **10**, 3254–3263.
- Lehrer, S. S. & Laevis, P. C. (1978) *Methods Enzymol.* **49**, 222–236.
- Lowry, O. H., Rosenbrough, N. J., Farr, A. L., & Randall, R. J. (1951) *J. Biol. Chem.* **193**, 265–275.
- Lunardi, J., Dupuis, A., Frobert, Y., Grassi, J., & Vignais, P. V. (1989) *FEBS Lett.* **245**, 223–228.
- Mac Lennan, D. H., & Tzagoloff, A. (1968) *Biochemistry* **7**, 1603–1610.
- Penin, F., Godinot, C., & Gautheron, D. C. (1979) *Biochim. Biophys. Acta* **548**, 63–71.
- Penin, F., Godinot, C., & Gautheron, D. C. (1984) *Biochim. Biophys. Acta* **775**, 239–245.
- Penin, F., Deléage, G., Godinot, C., & Gautheron, D. C. (1986) *Biochim. Biophys. Acta* **852**, 55–67.
- Schneider, E., & Altendorf, K. (1987) *Microbiol. Rev.* **51**, 477–497.
- Sternweis, P. C. (1978) *J. Biol. Chem.* **253**, 3123–3128.
- Tiedge, H., Lücken, U., Weber, J., & Schäfer, G. (1982) *Eur. J. Biochem.* **127**, 291–299.
- Tuttas-Dörschug, R., & Hanstein, W. G. (1989) *Biochemistry* **28**, 5107–5113.
- Walker, J. E., Runswick, M. J., & Saraste, M. (1982) *FEBS Lett.* **146**, 393–396.
- Walker, J. E., Fearnley, I. M., Gay, N. J., Gibson, B. W., Northrop, F. D., Powell, S. J., Runswick, M. J., Saraste, M., & Tybulewicz, V. L. J. (1985) *J. Mol. Biol.* **184**, 677–701.
- Walker, J. E., Runswick, M. J., & Poulter, L. (1987) *J. Mol. Biol.* **197**, 89–100.
- Williams, N., & Pedersen, P. L. (1986) *Methods Enzymol.* **126**, 484–489.
- Yoshida, M., Sone, N., Hirata, H., & Kagawa, Y. (1977) *J. Biol. Chem.* **252**, 3480–3485.